

Study experimental of the head flow geometry at front structures of sub-aqueous mudflow

Z. F. Haza and I. S. H. Harahap

Civil Engineering Department, Universiti Teknologi PETRONAS
Bandar Seri Iskandar, 31750 Tronoh, Perak, Malaysia

Abstract- Laboratory experiments were conducted to observe the front-flow structures of mudflow spreading under water in view of determining some aspects of the mass movement at the time of submarine slides. The mud used in this experiment consisted of 10-35% kaolin by weight and water. Several experiments were conducted using a simple technique of 'lock-exchange system' and gravity flow concept. The rheological properties of the mud were suitably fitted into the Herschel-Bulkley model. Flow velocity values were fluctuating. There was an acceleration-deceleration pattern, each mud models of 10% to 30% KCC (kaolin clay content) had a relative small fluctuation of velocity, whereas 35% KCC stopped at distance of about 2.3 m. The results indicate that density and yield strength govern the initial movement of the mudflow in terms of flow phase determination and flow front height evaluation.

Keywords: submarine slide; mudflow; kaolin clay; lock-exchange; gravity flow

I. INTRODUCTION

One of the geo-hazards which is well known as submarine slide is the phenomenon of failures within the seafloor that cause the displacement of seabed sediments. Recently, it has become a serious and complex problem in the marine field because it causes damages to the seabed environment and seafloor facilities. These events, are normally (in geological time scale) occurred in many areas around the continental margin, including slope instability, mud volcanoes and mudflows, gas hydrates, fluid seepage, bottom currents, and boulders.

Unconsolidated clays are the main material of seabed sediment deposits, which after collapse transform into a finely mixture of clay and water having properties of a non-Newtonian liquid. This movement represents the most effective process of sediment transport from the shallow continental margin into the deep ocean [1].

Several research and post-failure field observations have been conducted so far. One of the important characteristics derived from post-failure analysis data is that the submarine slides can reach very long run-out distance up to hundreds of kilometers on a gentle slope [1-4]. Other evidence obtained from field analysis is the majority of submarine slides involved cohesive fine-grained material, i.e. clays and silts [3]. Furthermore, some research characterized kaolin as the most predominant clay mineral contained in seafloor sediment [5-7]. That is in line with the findings that in terrigenous clastic sediment, muddy material dominated the schematic of sediment deposits [8].

Investigations of this study are focusing on the initiation of mudflow along an inclined channel by considering the front flow structures formation of mudflow at a certain time

and distance. The intention is to elaborate on the submarine slide initiation in terms of velocity, run-out distance, and the form of moving mass. Accordingly, this paper reports the implementation of a laboratory experiment for submarine slide simulation. This current experimental work was carried out the developing methods for the investigation of initial mud flow in submarine slides.

II. LABORATORY EXPERIMENTS

A. Laboratory setup

The muds, materials rich in clay, were the most susceptible material in submarine slides. Even though, there is no sediment deposit which contains only clay (as there are always sand and other coarser material), in this work, the effect of pure mud was studied, eliminating the effect of sand content.

In mudflows, the mechanics of movement cannot be adequately explained by soil mechanics principles alone thus applying fluid mechanics principles is necessary [9]. According to these principles, the analysis of flow behavior of submarine slide can be more appropriately studied using the gravity flow concept of fluid mechanics with a simple technique of generating gravity flow which was named 'lock-exchange system', which basically means separating two types of fluids having different densities in two chambers by vertical barrier. This method has been used in several fluid experiments including studies on fluid density factor [10-12] in which the effect of density ratio of two fluids have been investigated.

The simplicity of laboratory design is encouraging obtained results that could pave the way for further investigation of the characteristics of geophysical flows.

The facility for the laboratory was assembled at Hydrology Laboratory of Universiti Teknologi PETRONAS, Malaysia. The main equipment was a rectangular channel of 8.53 m length, 0.25 width, and heights of 0.7 m and 1.30 m at the beginning and end point, respectively.

The current experiment basically simulated a lump of mud, sliding into a pool of water then spreading over the surface of channel base. Fig. 1 shows the scheme of the experiment setup. The mud has density of ρ_f whereas, water has density of ρ_w , where $\rho_f > \rho_w$. The removable gate was removed rapidly to let the mud start flowing into the water. Mudflows were recorded using equipment of four fixed cameras: Fujifilm FinePix J10 8.2mp, positioned at 0.5 m after the gate location, while three cameras Sony Handycam HDR-HC-7e 6mp, positioned with a distance of 1 m respectively after the first camera.

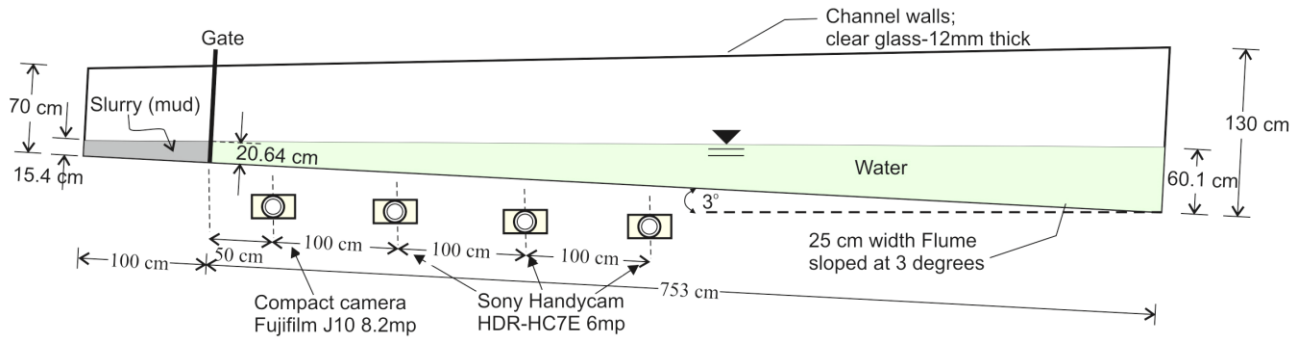


Figure 1. Schematic of the laboratory experiment setup

B. Material and rheological properties

The mud model was made from a mixture of refined kaolin (fabricated by the local kaolin industry of Malaysia) and water, with percentage variation of kaolin clay content (hereinafter abbreviated as KCC) in range 10% to 35%, with 5% increment. Kaolinite has a low shrink-swell capacity and a low cation exchange capacity (1-15 meq/100g.) and it is a soft and earthy with specific gravity (GS) value of about 2.6 and the density of kaolin is 2630 kg/m^3 , while water 1000 kg/m^3 .

Rheological test, including density and viscosity, was carried out by using common equipment in oil and gas industry, Fann Model 35 Viscometer and Mud Balance Model 140. This equipment was used primarily in the stage of drilling in the oil wells exploration process. The instruments and test kits were designed to conform to the testing standards established by the American Petroleum Institute (API) and published in API SPEC 10, API RP 10B-2, API SPEC 13A, API RP 13B-1, 13B-2, 13D, 13I, 13J, and 13K, and they were suitable for field and laboratory uses. An extended issue regarding time-dependency which has to be carefully monitored is when the slurries turns out to be rheopectic - a condition in which fluid viscosity increases with time. Thixotropic condition could also occur since clay-water mixture systems are well known as typical thixotropic material [13-14]. In order to complete and verify the rheology test results, mud models were re-tested using Brookfield Digital Viscometer DV-I+ equipment, according to ASTM D2196 [15].

According to the rheology of clay-water mixture, the experimental values in a wide shear rate ranges including values as small as 0.01 per second (or 0.01 s^{-1}) is fitted into the Herschel-Bulkley model. It also provides a theoretical yield stress which is very close to real yield stress, with a low level of uncertainty for conventional practical application [13]. Hence, mud rheological test are described using Herschel-Bulkley model to characterize its rheological behavior. Even though the linear viscoplastic Bingham model was the most commonly used to describe rheology of debris or mudflow, but the Herschel-Bulkley model has been found to be more appropriate for describing the nonlinear viscoplastic behavior of debris flows [16-17]. The Herschel-Bulkley model is expressed in the following equation.

$$(\tau - \tau_c) = K \cdot \dot{\gamma}^n \quad (1)$$

where, τ_c is the yield strength, K is equivalent to the dynamic viscosity, $\dot{\gamma}$ is the shear rate, and n is positive parameters of model factor [13]. Table 1 lists the mud models according to percentage of KCC. The densities and specific gravity values are obtained by rheological laboratory test then followed by Herschel-Bulkley models.

Based on the principles of gravity flow, density factor is important and closely considered for observations and analysis. The Boussinesq approximation may be applied regarding initial density ratios (ρ_i) in order to check the effects of density variations towards inertia. Initial density ratio is formulated as follow [18].

$$\rho_i = [(\rho_f - \rho_w) / (\rho_f + \rho_w)]^{1/2} \quad (2)$$

The mud model used for this experiment has value of ρ_i in range 0.17 to 0.27 for KCC below 25%, whereas 30% and 35% have value of 0.33 and 0.34, respectively. Furthermore, density ratios are calculated using equation of $\rho_r = \rho_w / \rho_f$ which is yielding values in range of 0.790 to 0.949, thus approaching these mudflows experiment using non-Boussinesq flow concept is possible [11].

C. Experiments Overview

Tracking the movement of mud flow is implemented by applying timeline feature (t), front velocity of head flow (u), and run-out distance (l).

TABLE I
RHEOLOGICAL TEST RESULTS AND HERSCHEL-BULKLEY MODEL

Percentage of KCC (%)	Density (ρ)		Specific Gravity (GS)	Herschel-Bulkley rheological model
	(lbs/gal)	(kg/m^3)		
10	8.79	1054	1.07	$\tau = 0.6 + 0.2 \dot{\gamma}^{0.3}$
15	9.1	1092	1.1	$\tau = 2 + 0.4 \dot{\gamma}^{0.3}$
20	9.45	1134	1.13	$\tau = 3.4 + 1.3 \dot{\gamma}^{0.32}$
25	9.6	1152	1.2	$\tau = 3.7 + 3.2 \dot{\gamma}^{0.4}$
30	10.3	1236	1.23	$\tau = 5.7 + 3.7 \dot{\gamma}^{0.42}$
35	10.55	1266	1.27	$\tau = 9 + 4.7 \dot{\gamma}^{0.5}$

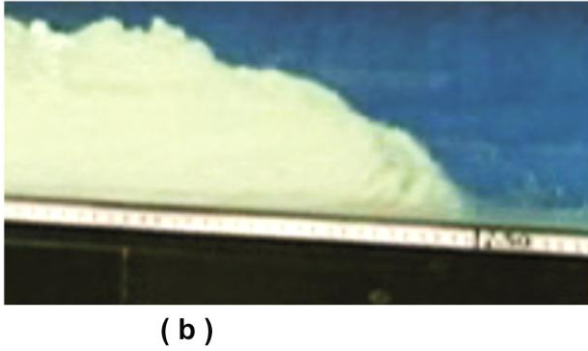
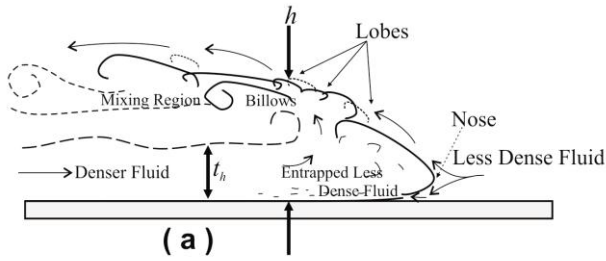


Figure 2. Head flow of gravity current; (a) Sketch of a typical gravity current front and its particular sections [19] (b) Image capturing of laboratory experiment

The velocity of the mudflow at certain flow-time and run-out distance is the reference point in the elaboration and examination of other flow aspects.

Gravity flow concepts describes the phenomena of stratified fluids when a denser fluid body spread under a less dense body of fluid [19]. In this case, mud was the denser fluid that flow under the water. Furthermore, the advance sketch of the typical gravity current front was provided as shown in Fig 2 below which has similarities with laboratory result.

Laboratory experiments were performed repeatedly three times for all percentage of KCC, in order to ensure the typical flow behavior of certain percentage. Analysis is using the average data among those experiments. Results show that there were similarities among three repetitions of each experiment.

There is conformity of the body shape of mudflow between experiment with sketch of typical gravity current in term of generating the main indicator of gravity current (i.e. lobes, billows and mixing region) as if dense fluid intruded into less dense fluid. Moreover, the chaotic interaction of flow regime on interface of mud and water is shown clearly. Further observation regarding interaction of these two stratified fluids will be related to Reynolds number, Re magnitudes which is formulated as the following.

$$Re_{non-Newtonian} = \frac{\rho_f \cdot u^2}{\mu_{app} \cdot \dot{\gamma}} \quad (3)$$

A very small wave in water surface were also generated by the flow, however, this phenomenon was not observed further since the water surface was definitely free surface condition.

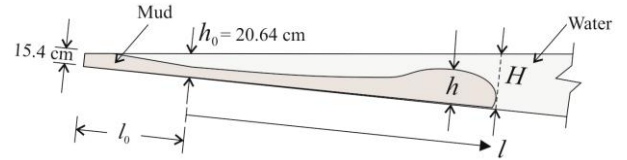


Figure 3. Schematic of the mudflow at $t > 0$ (i.e. during flow), equipped with details of flow structures

III. RESULT AND DISCUSSION

The details schematic of particular identification of mudflow at the start and during flow condition are facilitating the observation. In the initial condition has identification of $t = 0$, height, h_0 , and length, l_0 , those were measured as 0.2064 m and 1.00 m, respectively (see Fig. 1). Whereas, during flow condition, identification aspects are time (t), height of head-flow (h), water depth (H), and run-out distance (l) as displayed in Fig. 3 below.

As shown in Fig 1, once the gate was opened, it allowed the mud to perform movement by flowing across the channel base with shape of flow as sketched in Fig. 3. According to laboratory setup and numbers of percentage of KCC, Table 2 presents the list of experimental measurement results.

TABLE 2
FLOW MEASUREMENT RESULTS

Mud model	l (m)	t (s)	u (m/s)	h (m)	H (m)	Re
10%kcc~0.5	0.51	2.12	0.240	0.07	0.233	65.69
10%kcc~1	0.99	5.04	0.164	0.11	0.258	30.68
10%kcc~1.5	1.52	8.24	0.166	0.17	0.286	65.69
10%kcc~2.0	2.02	11.26	0.166	0.19	0.312	31.43
10%kcc~2.5	2.5	13.26	0.240	0.2	0.337	65.69
10%kcc~3	2.98	14.99	0.278	0.24	0.363	88.14
10%kcc~3.5	3.47	16.71	0.285	0.25	0.388	92.64
15%kcc~0.5	0.47	1.90	0.248	0.07	0.231	25.26
15%kcc~1	0.98	4.11	0.230	0.1	0.258	21.89
15%kcc~1.5	1.5	6.24	0.244	0.16	0.285	24.53
15%kcc~2.0	1.97	8.94	0.174	0.17	0.310	12.52
15%kcc~2.5	2.48	11.01	0.246	0.19	0.336	25.02
15%kcc~3	3.01	13.14	0.249	0.22	0.364	25.52
15%kcc~3.5	3.5	15.12	0.248	0.23	0.390	25.26
20%kcc~0.5	0.5	1.14	0.439	0.07	0.233	39.20
20%kcc~1	1.03	3.33	0.242	0.08	0.260	11.91
20%kcc~1.5	1.47	5.80	0.179	0.13	0.283	6.52
20%kcc~2.0	2	7.99	0.242	0.15	0.311	11.91
20%kcc~2.5	2.5	9.95	0.255	0.16	0.337	13.22
20%kcc~3	3.03	12.06	0.251	0.19	0.365	12.81
20%kcc~3.5	3.54	13.93	0.274	0.21	0.392	15.27
25%kcc~0.5	0.5	1.14	0.439	0.07	0.233	22.67
25%kcc~1	1.05	3.36	0.248	0.1	0.261	7.24
25%kcc~1.5	1.53	5.13	0.271	0.12	0.287	8.64

25%kcc-2.0	2	7.01	0.250	0.14	0.311	7.35
25%kcc-2.5	2.49	9.04	0.256	0.15	0.338	7.71
25%kcc-3	2.9	10.54	0.254	0.16	0.358	7.59
25%kcc-3.5	3.5	12.85	0.259	0.17	0.390	7.89
30%kcc-0.5	0.48	1.17	0.410	0.08	0.232	16.30
30%kcc-1	1	3.47	0.226	0.09	0.259	6.45
30%kcc-1.5	1.47	5.51	0.230	0.1	0.283	9.75
30%kcc-2.0	1.98	8.33	0.181	0.1	0.310	4.14
30%kcc-2.5	2.51	10.00	0.317	0.09	0.338	5.13
30%kcc-3	3	11.94	0.253	0.09	0.364	8.08
30%kcc-3.5	3.5	13.93	0.251	0.09	0.390	7.95
35%kcc-0.5	0.54	1.25	0.431	0.08	0.235	13.10
35%kcc-1	0.98	3.76	0.175	0.07	0.258	2.11
35%kcc-1.5	1.52	5.97	0.226	0.08	0.284	3.60
35%kcc-2.0	1.98	15.86	0.051	0.08	0.310	0.18

Table 2 shows a significant effect of the rheology factors of the yield strength (τ_c) on the structures of head flow formation and run-out distance of the mudflow. The percentage increments of KCC (i.e. 10 to 35%) increase τ_c , but, on the other hand, reduce the height of head flow, h . Obviously, the high value of τ_c of 35% KCC is also likely to lead the short run out distance, l , at distance of 2.51 m.

The basic fluid mechanics principles described that a flow is regarded as turbulent when the R_e is high. Hence, values of R_e in Table 2 were calculated using (3) confirming that small KCC has high R_e which generate more chaotic flow surface (i.e. more lobes and billows, wider mixing region, and higher head flow height).

The propagation of head velocities during flow, starting from gate point until distance of 3.5 m are shown in Fig. 4. It is the flow behavior as viewed from the mudflow velocity and run-out distance. It can be seen that there was a pattern of acceleration and deceleration of the flow. Each mud models of 10% to 30% KCC had a relative small fluctuation of velocity in range of $l_{1,0}$ to $l_{3,5}$, whereas 35% KCC underwent a rapid deceleration to stop at around $l_{2,3}$.

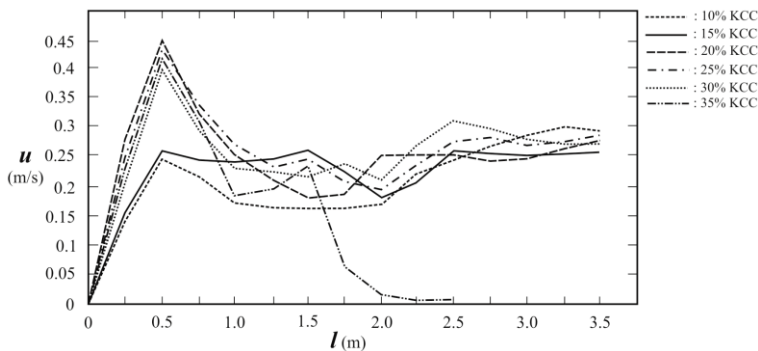


Figure 4. Head-flow velocities as a function of run-out distance in range of 0 to 3.5 m

There are three flow phases of flow in reference to propagation velocities and run-out distance, those are slumping phase, inertial-buoyancy phase, and viscous buoyancy phase [18, 20-21]. Furthermore, balancing force difference provides a specific rate of spreading for characteristics of each flow phase. Further observation, the position of flow front is traced by plotting time, t , versus run-out distance, l , in order to relate the effect of acceleration-deceleration pattern against flow. Plotting graphs are implemented by non-dimensional length unit of η and non-dimensional time unit of (t / t_0) . The axis of η is formulated as l / l_0 , with respect to initial length of mud deposit, l_0 , whereas (t / t_0) with respect to t_0 which is formulated as $t_0 = l_0 / (g'h_0)^{1/2}$.

The effect of acceleration-deceleration pattern can be seen in Fig. 5 that the graphs do not display straight line from beginning to the end point - there are some break points along the line. This condition indicates that the mudflow velocities are not linear which are similar with the graph of velocity versus run-out distance as shown in Fig 4.

According to three phases of flow, the gray area displayed in Fig 4 is the area of slumping phase since this phase is identified by the magnitude of slope of $[\eta / (t / t_0)]$ which is equal to 1 [18]. Based on this figure, it is confirmed that plotting lines of 10 to 25% KCC get slope magnitude of $[\eta / (t / t_0)]$ greater than 1 while 30% KCC gets ~ 1 . The 35% KCC shows the different trend line, part of its line is inside gray area and the rest is outside with slope magnitude of ~ 0.25 which can be considered as viscous buoyancy phase. It can be concluded in this current experiment that the mudflows of 10 to 30% KCC were still performing in the initial slumping phase, whereas the 35% KCC overstepped two phases of initial slumping and viscous buoyancy phase.

The increment of front height (h) mudflow, according to Table 2, can be monitored during motion with run-out distance (l). The growth of h is the result of two distinct mechanisms between mud and water. Thereafter the front heights listed in Table 2 are plotted in graph with axis of non-dimensional length of η , as shown in Fig.6.

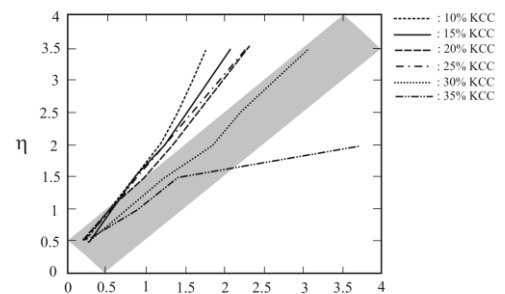


Figure 5. Plots of the run out distance (i.e. front flow position) as a function of time for each percentage of KCC

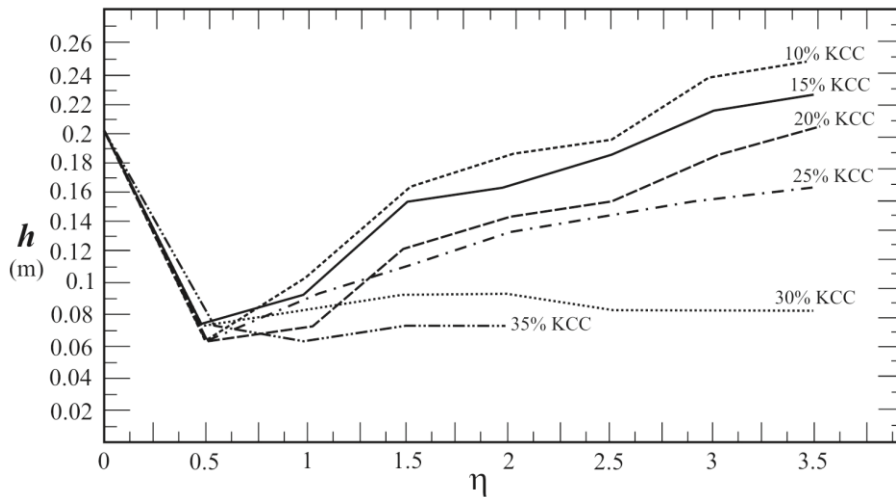


Figure 6. Flow-front height as function of non-dimensional length η

IV. CONCLUDING REMARK

Experimental work of mudflow was conducted on sloping base under water to observe some characteristics of submarine slides. The characteristic rheological properties were described satisfactorily using both Brookfield Digital Viscometer DV-I+ and Herschel-Bulkley rheological model.

Flow velocity values were fluctuating at initial run-out. They had an acceleration-deceleration pattern, each mud models of 10% to 30% KCC had a relative small fluctuation of velocity in range of $l_{1.0}$ to $l_{3.5}$, whereas 35% KCC stopped at around $l_{2.3}$. According to velocity analysis based on Fig. 4, it can be inferred that in range from l_0 to $l_{3.5}$ run-out distance, mudflows experienced initial slumping phase, and 35% KCC overstepped two phases of initial slumping and viscous buoyancy phase.

The work indicates that mud density and yield strength can be used to predict flow head geometry at any time and distance from slide source, as such; it can be used as a basis to predict mud flow impact on various seabed structures some distance in its vicinity.

Future work would be improved the quality of visually observations by using advanced equipment for tracking mud particles during motion. In addition, it is important to develop a quantitative verification through numerical simulation in order to accommodate the initial and boundary conditions of mudflow in research.

ACKNOWLEDGMENT

This research was also part of the Graduate Assistantship Scheme (GA-Scheme) of Universiti Teknologi PETRONAS Malaysia.

REFERENCES

[1] F. V. D. Blasio, *et al.*, "Hydroplaning and submarine debris flows," *Journal of Geophysical Research*, vol. 109, pp. 1-15, 2004.

[2] A. Elverhoi, *et al.*, "On the dynamics of subaqueous debris flows," *Oceanography*, vol. 13, pp. 109-117, 2000.

[3] J. J. Hance, "Development of a Database and Assessment of Seafloor Slope Stability based on Published Literature," Master of Science in Engineering, Faculty of the Graduate School, The University of Texas, Austin, 2003.

[4] P. Bryn, *et al.*, "Explaining the Storegga Slide," *Marine and Petroleum Geology*, vol. 22, pp. 11-19, 2005.

[5] A. E. Fallick, *et al.*, "Implications of linearly correlated oxygen and hydrogen isotopic compositions for kaolinite and illite in the Magnus Sandstone, North Sea," *Journal of Clays and Clay Minerals*, vol. 41, pp. 184-190, 1993.

[6] J. S. Youn, *et al.*, "Sedimentary Strata and Clay Mineralogy of Continental Shelf Mud Deposits in the East China Sea," *International Journal of Oceans and Oceanography*, vol. 1, pp. 183-194, 2006.

[7] C. Martín-Puertas, *et al.*, "A comparative mineralogical study of gas-related sediments of the Gulf of Cádiz," *Geo Marine Letter*, vol. 27, pp. 223-235, 2007.

[8] G. Nichols, *Sedimentology and Stratigraphy*. Oxford, 1999.

[9] J. Locat and H. J. Lee, "Submarine Landslides: Advances and Challenges," presented at the The 8th International Symposium on Landslides, Cardiff, U.K, 2000.

[10] J. O. Shin, *et al.*, "Gravity currents produced by lock exchange," *Journal of Fluid Mechanics*, vol. 521, pp. 1-34, 2004.

[11] R. J. Lowe, *et al.*, "The non-Boussinesq lock-exchange problem. Part 1. Theory and experiments," *Journal of Fluid Mechanics*, vol. 537, pp. 101-124, 2005.

[12] V. K. Birman, *et al.*, "Lock-exchange flows in sloping channels," *Journal of Fluid Mechanics*, vol. 577, pp. 53-77, 2007.

[13] P. Coussot, *Mudflow Rheology and Dynamics*. Rotterdam: AA Balkema, 1997.

[14] A. Zakeri, *et al.*, "Submarine debris flow impact on pipelines — Part I: Experimental investigation," *Coastal Engineering*, vol. 55, pp. 1209 - 1218, 2008.

[15] Standards, "ASTM D1092-05 Standard Test Methods for Rheological Properties of Non-Newtonian Materials by Rotational (Brookfield type) Viscometer.," ed: ASTM International, 2005.

- [16] N. J. Balmforth, *et al.*, "Shallow viscoplastic flow on an inclined plane," *Journal of Fluid Mechanics*, vol. 470, pp. 1-29, 2002.
- [17] S. Cohard and C. Ancey, "Experimental investigation of the spreading of viscoplastic fluids on inclined plane," *Journal of Non-Newtonian Fluid Mechanics*, vol. 158, pp. 73-84, 2009.
- [18] L. A. Amy, *et al.*, "Abrupt transitions in gravity currents," *J. Geophys. Res.*, vol. 110, pp. 1-19, 2005.
- [19] K. M. Mok, *et al.*, "Experimental Observations of The Flow Structures at Gravity Current Fronts," presented at the International Conference on Estuaries and Coasts, Hangzhou, China, 2003.
- [20] H. E. Huppert and J. E. Simpson, "The slumping of gravity currents," *Journal of Fluid Mechanics*, vol. 99, pp. 785-799, 1980.
- [21] J. W. Rottman and J. E. Simpson, "Gravity currents produced by instantaneous releases of a heavy fluid in a rectangular channel," *Journal of Fluid Mechanics*, vol. 135, pp. 95-110, 1983.